Geophys. J. R. astr. Soc. (1974) **38,** 237–251.

Numerical Modelling of Tectonic Flow behind Island Arcs

D. J. Andrews* and N. H. Sleep†

(Received 1974 May 15)‡

Summary

High heat flow in marginal basins and island arc volcanism are explained by numerical modelling of flow induced by the downgoing slab. The hypothesis that frictional heating above the slab causes thermal diapirs to rise is mechanically unfeasible since the region above the slab must be fluid enough to convect thermally, yet so viscous that the motion of the slab produces over 2 kilobars of stress. The calculation of induced flow is two-dimensional, time dependent, with a variable viscosity dependent on temperature and pressure. A yield stress was used to approximate fault dislocations. The calculation is very sensitive to the material properties and to localized flow near the base of the interface between the slab and the landward plate. The highest stress occurred at the base of the slab interface. This area ablated creating a narrow channel necessary for separating melt from mostly crystalline mush to establish a source of volcanic magmas. In the marginal basin area, tensile yielding occurred in the plate causing it to thin and raise the heat flow significantly. The yielding continued until a complete rift occurred. Induced flow is, then, a likely explanation for island arc volcanics and high heat flow in marginal basins.

Introduction

The association of volcanic island arcs with sites of presumed subduction of oceanic crust is well established. Marginal basins, floored by young oceanic crust, often occur landward of the volcanic arc. The Sea of Japan, the Sea of Okhotsk, the Lau-Havre Basin, the Andaman Sea and the Tyrrennian Sea are examples of these basins. Bulk upwelling of material from the asthenosphere to the lithosphere induced by the motion of the slab or other tectonic stresses is a possible explanation for island arc volcanics and marginal basins (Isacks, Oliver & Sykes 1968; Gorshkov 1969, 1970) which has received little attention since it is difficult to model. The purpose of this paper is to investigate this induced motion with numerical calculations. The work is motivated, in part, by serious difficulties with other hypotheses for explaining island arc volcanism and intra-arc basins which are described below.

* Now at US Geological Survey, Menlo Park, California 94025.

† Now at Northwestern University, Evanston, Illinois 60201.

‡ Received in original form 1973 December 8.

The hypothesis that subducted sediments, by their lower melting temperature, are responsible for volcanism, is disputed by two observations. Inclusion of subducted material in island arc volcanics cannot be demonstrated from geochemical data (Oversby & Ewart 1972), and the eruption temperature, and therefore probably source temperature, of island arc volcanics is similar to that of basalts from other regions (Osborn 1969).

The commonly proposed mechanism of frictional heating on the fault plane above the slab is not, by itself, a satisfactory process for island arc volcanism or the observed high heat flow in marginal basins. As the slab provides a heat sink, shear stress of at least 2 kb (compared with apparent stress drops of less than 100 bars in subduction zone earthquakes (Molnar & Wyss 1972) is needed to produce a local thermal maximum even in the most optimistic calculations (Minear & Toksöz 1970a; Toksöz, Minear & Julian 1971; Hasebe, Fujii & Uyeda 1970; Turcotte & Schubert 1973). Extensive material transport is necessary for this frictional heat to produce the observed high surface heat flow in marginal basins since thermal conduction is too slow. (McKenzie & Sclater 1968; and above references).

An extensive zone of hot material beneath many island arcs inferred from seismic observations (Utsu 1971), high heat flow (Matsuda & Uyeda 1971), high temperature metamorphism (Oxburgh & Turcotte 1971; Matsuda & Uyeda 1971) and eruption of rhyolites produced by partial melting in the crust (McBirney & Weill 1966; Pushkar, McBirney & Kudo 1972) would greatly reduce frictional heating since the low viscosity of hot material would reduce stress. This inference is supported by the observation that great thrusting earthquakes are less frequent in regions where hot material is inferred to exist between the crust of the arc and the slab (Kanamori 1971). Other physical problems in producing a large hot region by frictional heating are the requirement that high stresses occur over large regions and the requirement that the region be able to convect under small temperature contrasts, yet resist the descent of the slab enough to produce the frictional heating (see Appendix I).

Geophysical model

Idealized diagrams of subduction zones generally show the top of the slab as a sharp interface with the lithosphere of the island arc and with the asthenosphere. In actuality the slab must interact and produce at least some deformation or induced flow in adjacent regions. We consider three types of such interactions: (1) Flow in the wedge of asthenosphere between the slab and the lithosphere of the island arc; (2) Entrainment of part of the lithosphere of the island arc by the slab and recharge of material from the asthenosphere to take its place; (3) Rifting of the lithosphere behind the island arc due to tension from the processes above. The second process, which acts over a smaller distance than the third process, is discussed in connection with island arc volcanism. The third process is discussed in connection with intra-arc spreading.

An analytic solution is available for flow in a wedge-shaped region, such as between the slab and the lithosphere of the arc (Batchelor 1967; McKenzie 1969). This solution is most easily given in terms of a stream function defined such that

$$\text{curl } \vec{S} = \vec{V}$$

where

$S = |\vec{S}|$ = stream function

$\vec{V}$ = velocity.

The relevant solution for the asthenosphere landward of the slab is

$$S = \frac{rv[(\theta_d - \theta)\sin\theta_d \sin\theta - \theta_d \theta \sin(\theta_d - \theta)]}{\theta_d^2 - \sin^2\theta_d}$$

where

r = distance from slab-lithosphere corner,

v = subduction rate,

θ = dip angle measured about pole at $r = 0$ and from horizontal,

θ_d = dip of slab.

This solution provides a general idea of the expected flow pattern, but is singular, because the stress components are inversely proportional to the first power of the distance from the corner of the wedge. The infinite stress at the corner is obviously unrealistic and one should expect either a change in the flow pattern or non-linear viscosity to remove the singularity. Away from the corner, plausible stresses result. For example, for a wedge angle of 45°, with an asthenosphere viscosity of 10^{21} poise, and a slab velocity of 10 cm/yr, the induced flow in the asthenosphere exerts a shear stress on the plate above of 82 bars at a distance of 100 km from the corner. When a rigid lower boundary is assumed to exist at the base of the asthenosphere, a series of eddies occurs with maximum tension at the divergent point of the first eddy (Sleep & Toksöz 1971). There is no preferred point of tension in the wedge solution.

Models which consider only the asthenosphere have the fundamental problem that the solutions are singular in the corner of the slab with the horizontal lithosphere. If induced flow is to be related to volcanism, an improved model is needed because volcanic arcs occur directly over that location. One would expect a transition layer between the asthenosphere and the lithosphere. Due to the large stresses in this corner, the material from the transition layer could be entrained with the asthenosphere flow. The region ablated in this fashion could be the source for island arc volcanism. The region would be of small spatial extent with large stress gradients. There would be a continuous flow of mantle material through the region, and material upwelling into the region would have an increased fraction of melt. These are the conditions required to segregate magma from a mostly crystalline partial melt (Sleep 1974). The segregated magma could ascend to the surface by a local intrusion process (Weertman 1971).

For this process to be viable it is necessary that the new material which upwells, move fast enough that it circulates before it cools. The following dimensional analysis indicates that this is not a severe constraint. The time for the material to cool,

$$l^2/\kappa,$$

where

l = length scale,

κ = thermal diffusivity,

can be equated with the time of circulation,

$$l/V,$$

where

V = velocity,

to obtain a minimum necessary velocity. For $l = 10$ km and $\kappa = 10^{-2}$ cm^2 s^{-1} this velocity is 0·3 cm/yr. Thus any entrainment of material from the lithosphere at a significant fraction of the subduction rate could create a zone of increased temperature. The numerical models presented below attack the mechanical aspects of this problem.

The idea that the descent of the slab may create local tension beneath the arc allowing the asthenosphere to upwell passively to form intra-arc basins has been frequently suggested (Holmes 1965; Isacks *et al.* 1968; Kraus 1971; Sleep & Toksöz 1971), but only crudely modelled. Although this process occurs over a larger region than the entrainment process discussed above, it is still necessary to explicitly consider the lithosphere of the arc. The stress state in the landward plate is determined first, by the drag on the base of the plate from the induced flow, and secondly, by the stress along the fault plane. Define a co-ordinate system with the x-axis horizontal, normal to the strike of the trench. Let s_{xx} and s_{xy} be stress deviator components with s_{xx} positive in tension. A shear stress of 1 kb on the fault, acting alone, would produce a uniform stress state of $s_{xx} = -1$ kb, $s_{xy} = 0$. This uniform horizontal compression would work against both volcanism and marginal basin spreading. To this we must superimpose the stress produced by the induced flow. The induced flow will contribute a stress field which has horizontal tension, with this tension increasing as the distance increases from the corner.

By balancing forces on a segment of the plate, one can see that the horizontal stress deviator averaged through the thickness, l, of the plate will be $s_{xx} = (1/l)\int s_{xy}\,(\text{wedge})\,dx$. The integral does not exist for the wedge solution because the stress is singular at the corner. From this observation we can conclude that the overall stress solution can be quite sensitive to the detailed flow and rheology at the corner. This idealized stress analysis is a guide for understanding the numerical results; not an input to our calculations.

Once tension starts to neck or rift the lithosphere at a particular location, further yielding will tend to concentrate there. If the spreading is fast enough, hot material can ascend from the asthenosphere to near the surface. A feature formed thusly would have heat flow and topography similar to a mid-ocean ridge. Much data indicates that spreading in intra-arc basins does resemble a mid-ocean ridge (e.g. Karig 1971; Sclater, Ritter & Dixon 1972). As with ridges, however, the data which establish spreading are of little use in appraising mechanisms that induce spreading.

Calculations

Our calculation of induced flow beneath the landward plate is time dependent and two-dimensional. The motion of the slab is imposed as a boundary condition on the calculational region (see Fig. 1). The slab dipped at 45° and was given a velocity of 10 cm/yr. The high velocity was chosen in order to maximize the effects of induced flow. The fluid at the slab boundary must either move at the prescribed slab velocity or be at a shear stress of 1 kb, the maximum shear stress allowed on the fault. The fluid in the interior of the grid is considered to have a variable viscosity dependent on temperature and depth. In this manner the asthenosphere and lithosphere are treated as a single fluid. The calculational method is that developed by Andrews (1972) (see Appendix II). The landward plate is fixed at the left boundary and is free on the top boundary. Below 80 km on the left and bottom boundaries, the analytic solution for induced flow in a wedge (see equation (1)) is imposed.

The initial temperature distribution in the calculational region is uniform horizontally, and has a vertical gradient determined by a conductive heat flow of $1{\cdot}1\mu$ cal cm^{-2} s^{-1} above 80 km and an adiabatic gradient below 80 km. This initial temperature field is not, of course, in a conductive steady state. We are depending on circulation below 80 km to transport heat upward to maintain plate thickness. At

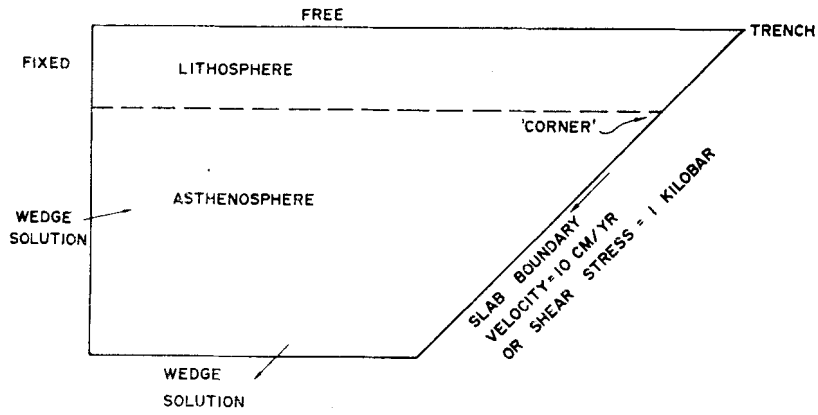

FIG. 1. Schematic diagram of the calculational region, indicating boundary conditions.

distances larger than 500 km from the slab, the plate does indeed thicken slowly as the solution progresses in time. Closer in, the lithosphere can become thinned. The conductivity used is 0·0075 cal cm^{-1} s^{-1} deg^{-1}.

A thermally activated viscosity was used with the functional form,

$$\eta = \eta_0 \exp \frac{E^* + PV^*}{RT} .$$

The value of the activation energy, E^*, used was 50 kcal per gram-atom. A low value was chosen to get a gradual transition between lithosphere and asthenosphere. The activation volume was $V^* = 1{\cdot}5\ cm^3$/gram-atom, such that viscosity does not change on an adiabat. This value was chosen for convenience, to have a constant viscosity in the asthenosphere. The constant η_0 was chosen to give $\eta = 10^{21}$ poise in the astheno-

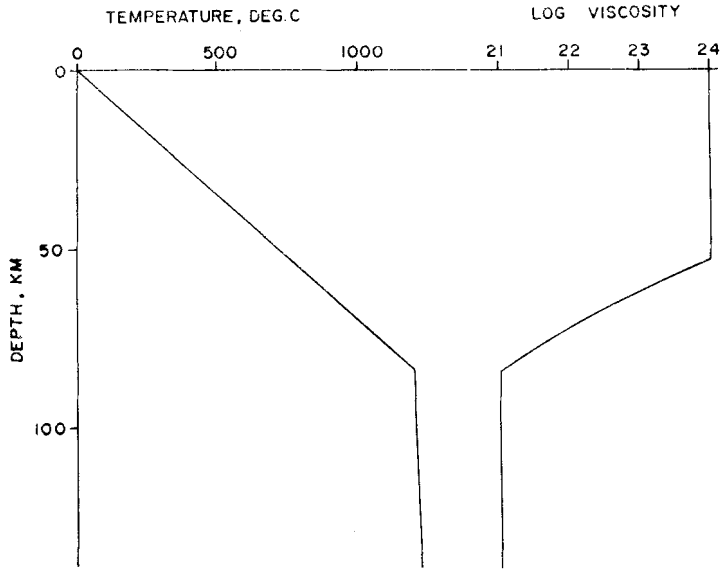

FIG. 2. Temperature and viscosity in the initial, laterally uniform, state.

sphere. In the lithosphere, there is a gradual decrease in temperature and consequent increase in viscosity by a factor of 10 in 10 km, as one approaches the surface (see Fig. 2). To avoid numerical problems, an upper limit on viscosity of 10^{24} poise was imposed. There is no lower boundary to the asthenosphere in these models.

The first calculation, which assumed yield stress on the fault but no yield stress in the interior of the grid, produced ridiculous results. At the slab, a cool boundary layer formed with a high viscosity. This layer was attached to the plate above and was not free to move at the slab velocity. The fault stress of 1 kb added up to give a considerable tension at the point where the boundary layer was attached to the landward plate. Clearly, this cold layer should break off and move down with the slab. To achieve this reasonable result, we must introduce a yield stress. The use of one complication, temperature-dependent viscosity, forces us to another complication in the model, a yield stress. Even though we would like to keep things simple, we are forced to use at least this kind of non-linear rheology.

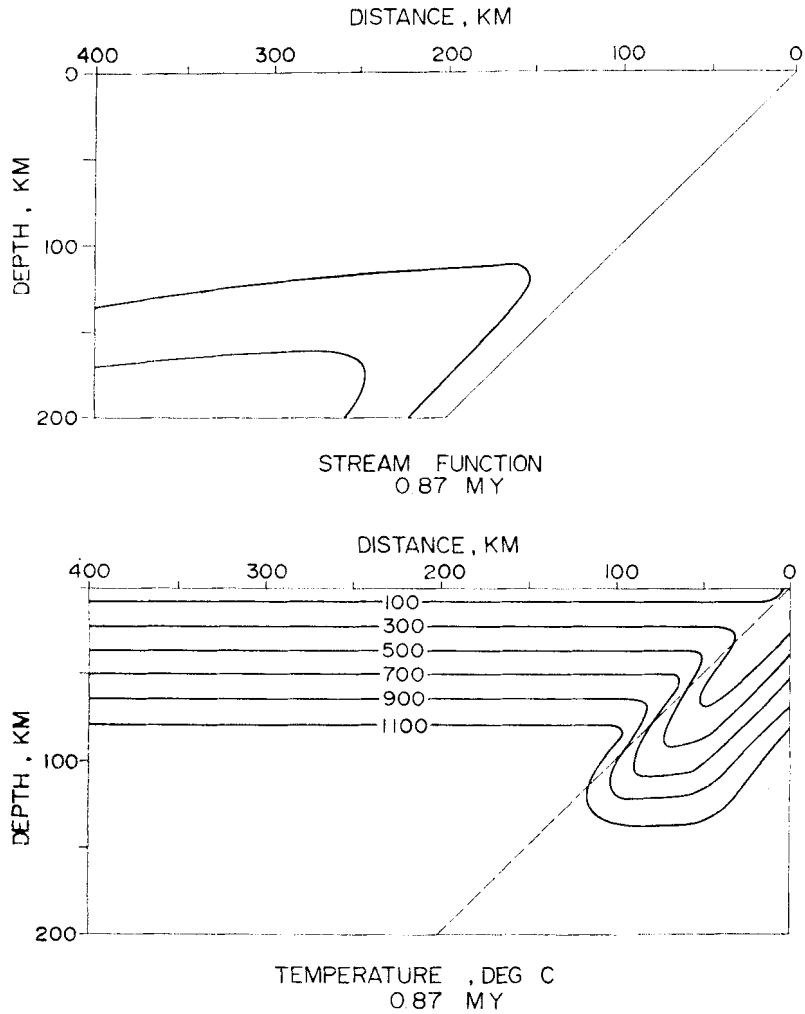

FIG. 3. Streamlines and isotherms at 0·87 My from start of subduction.

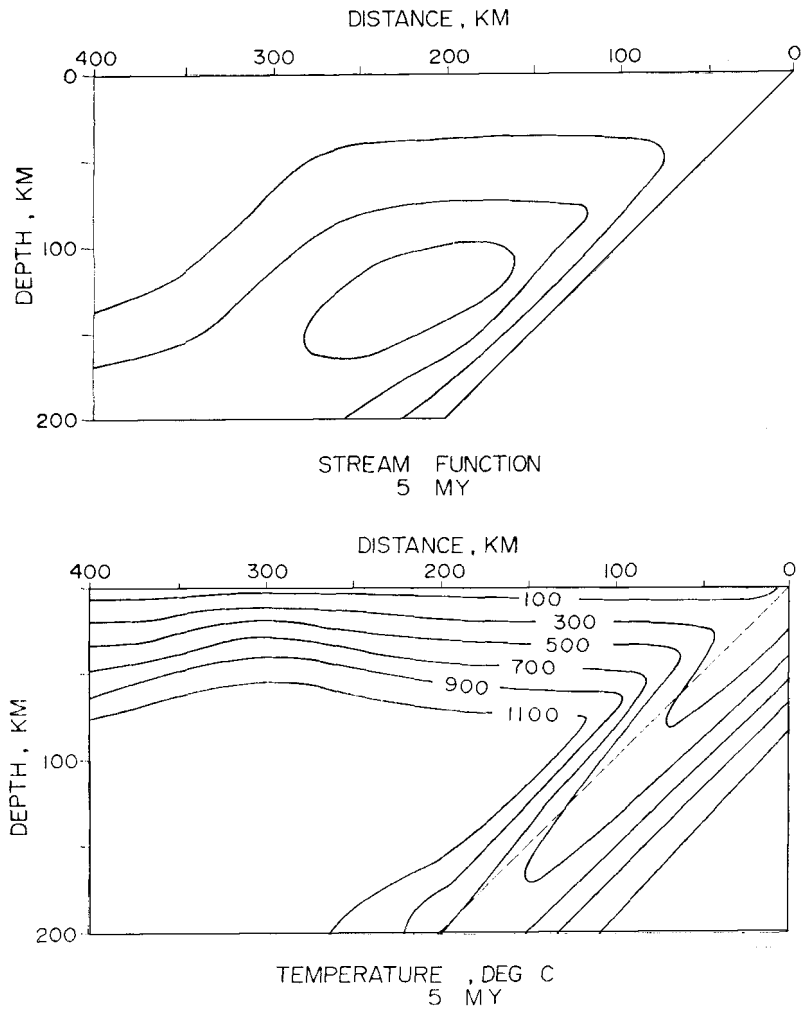

FIG. 4. Streamlines and isotherms at 5 My.

The next calculation, which was done with a yield stress in the interior of the region equal to 4 times the yield stress on the fault, produced little improvement. Yielding occurred only in a small region at the corner. In this case, the plate got thicker and the corner filled in with lithosphere as the calculation progressed. This, of course, contradicts observations of the island arc area. These results contrast strikingly with those obtained with lower yield stress.

The calculations that will be shown in detail were done with the yield stress equal to 1 kb both on the fault and in the interior of the region. This is equivalent to assuming that the shear stress required to make new breaks is the same as shear stress required for sliding on old breaks. For large volumes of material over long periods of time, this may be reasonable. Since there is no preferred plane of weakness specified at the beginning, that particular artificiality has been removed, except for boundary conditions on the grid.

What is to be observed in this calculation are deviations from Batchelor's wedge solution. In this case, it is important to observe whether the features of the solution

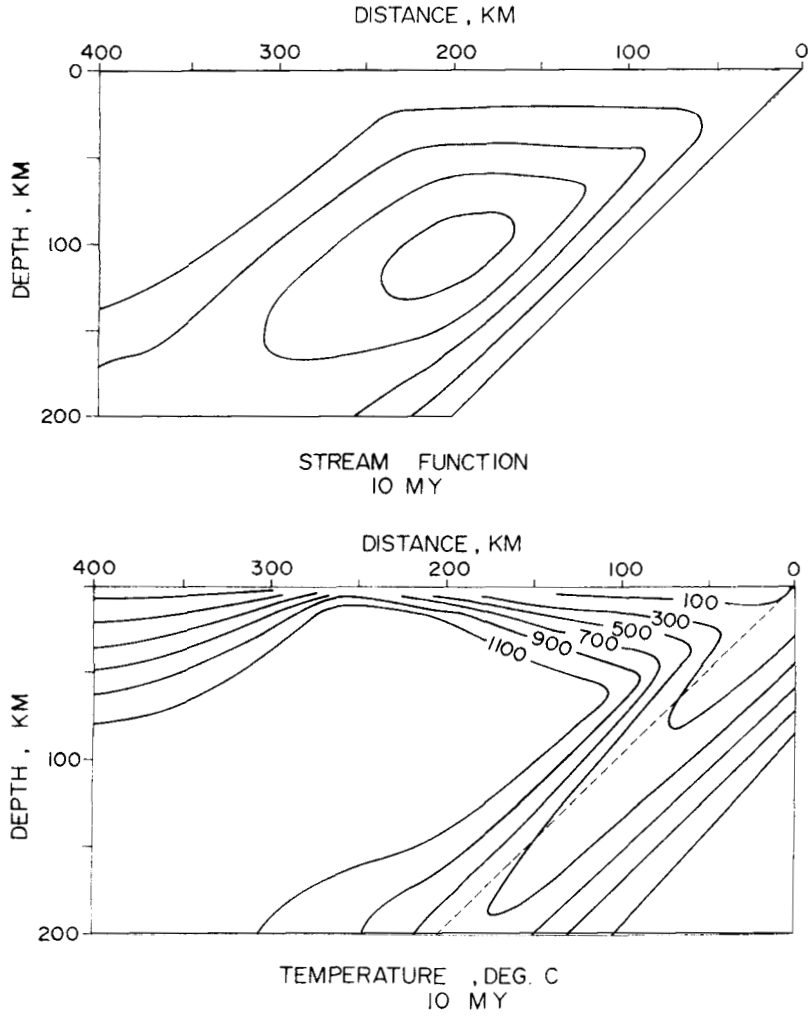

FIG. 5. Streamlines and isotherms at 10 My.

are determined by artificialities in the boundary conditions. Also, we can expect that very localized processes can be important. A re-zoning procedure was needed to check these problems and still conserve our computer resources. The calculation was started with a grid extending 800 km from the trench and extending to a depth of 400 km with zones 20 by 20 km. The wedge solution was imposed on the boundary of the asthenosphere. After running the problem 0·1 My, the solution on the coarse grid was remapped to a finer grid extending to 400 km width and to 200 km depth. Boundary values for stream function were taken from the coarse solution. So far the plate on top is nearly rigid. The horizontal stress near the trench is compressive and a region aligned along the dip of the fault approximately 30 km wide is yielding. Farther away, the horizontal stress becomes tensile and increases up to 250 bars at 400 km.

As the details of flow near the corner change, we should expect changes also in the horizontal stress in the plate above. As time progresses, the stress becomes more tensile until at about 1 My yielding starts at 330 km from the trench. Streamlines

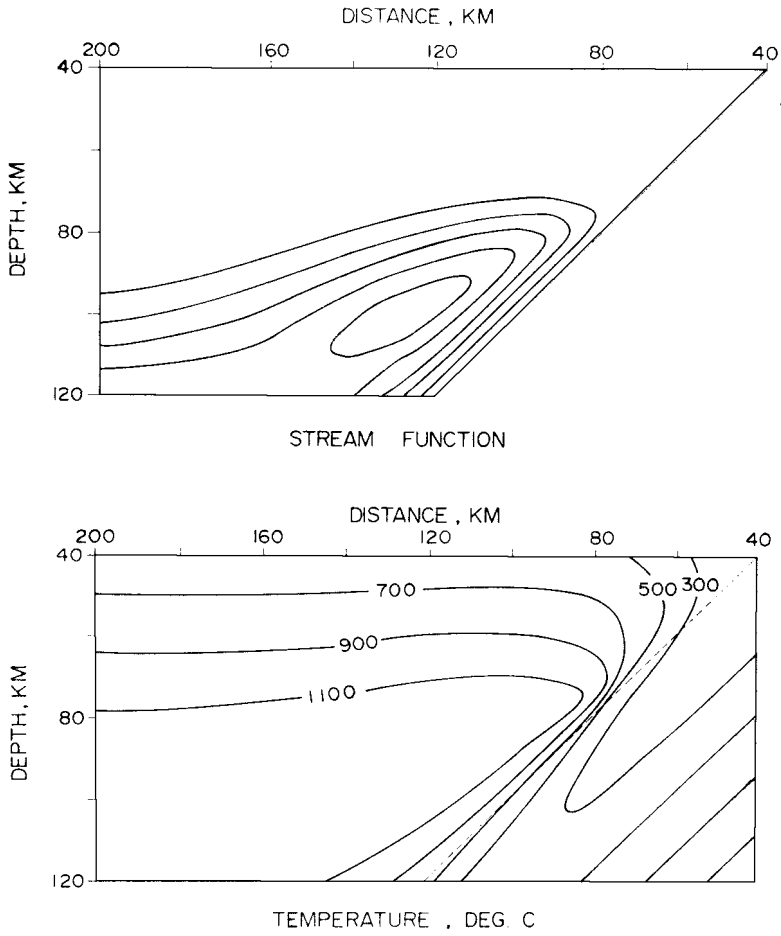

FIG. 6. Results of the calculation with finer resolution at 4 My showing ablation in the corner region.

and isotherms at that time are shown in Fig. 3. As time proceeds yielding continues, and the lithosphere necks down in the region where yielding started. Streamlines and isotherms at 5 My are shown in Fig. 4. In the necking region the lithosphere has thinned by 23 km. The portion of the plate between the neck and the slab is moving toward the slab at a gradually increasing velocity which, at 5 My, is 2·6 cm/yr.

The location of this rifting is determined by stress on the fault and by drag stress on the base of the plate. The drag is proportional to the viscosity of the asthenosphere and to the slab velocity. If yield stress and viscosity were scaled together, neither the stream function nor the location of the rifting would change. If the yield stress alone were decreased, rifting would start closer to the corner.

In view of the uncertainties of the physical parameters and of the sensitivity to the solution at the corner, the location of the rifting is not well determined. What we are demonstrating here is that significant rifting can take place without the use of unreasonable parameters.

As this tensile yielding continues, a true rift develops separating the plate into two pieces—something like a mid-ocean ridge. The portion of the plate near the trench is being subducted in the region of yielding there. Fig. 5 shows streamlines and isotherms at 10 My. The spreading is well advanced and the little portion of the plate,

now moving 4·4 cm/yr, is largely swept away leaving warm material up close to the surface. The surface heat flow in the calculation is as large as 10 times the normal value. In nature, local intrusions could considerably increase and scatter measured values. Although this is not a unique model, there is clearly no difficulty explaining high heat flow in marginal basins.

The finding that a considerable portion of the landward plate is subducted, calls into question the prescription of a location for a fault. It would be desirable to consider the oceanic plate as part of the problem, since no rigid 'hinge' exists at the turning point of the oceanic plate. Such work is in progress by one of the authors (N.S.). Two-sided subduction is obtained. It is perhaps essential to include the lower density of the island arc crust to achieve the one-sided subduction observed in nature (McKenzie 1969).

In order to look at ablation, one would want to go through a sequence of re-zonings quickly in order to get down to fine resolution at an early time. However, in order to look at the marginal basin spreading, we could not rezone to a grid smaller than 400 km. Unfortunately, this requires separate calculations for ablation and spreading. The ablation calculation was done with a zone size of 4 km. The top of the grid is at 40 km depth and the bottom at 120 km, starting with a horizontally uniform temperature. The top boundary was fixed, preventing any stretching of the plate. In this calculation, resolution is fine enough to see effects with a length scale of the thickness of the transition layer.

In this calculation, significant ablation is produced. The material from the transition zone is entrained with the flow of the asthenosphere as is shown in Fig. 6. At 4 My, the streamlines rise 30 km. Ablation is more rapid in the first 2 My than between 2 and 4 My, and would probably proceed quite slowly thereafter. The ablation extends only a small fraction of the way through the plate and over a small horizontal distance.

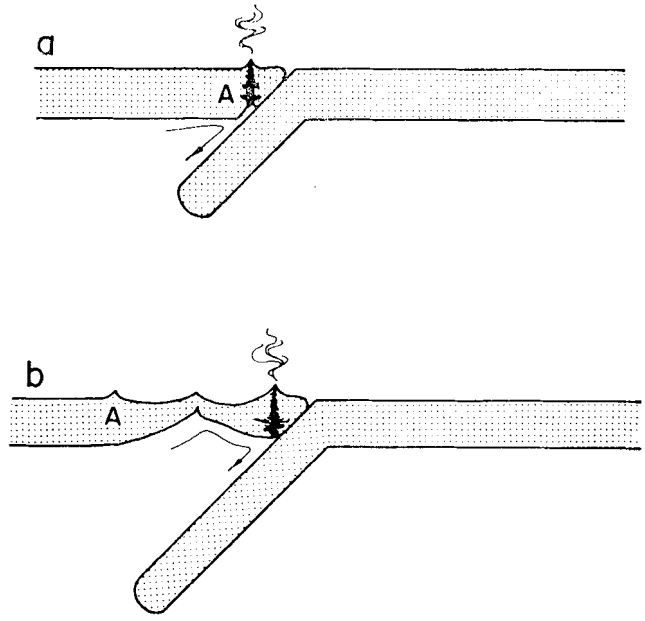

FIG. 7. A schematic model. Spreading in the marginal basin is symmetric, and starts at the volcanic intrusion. No part of the island-arc plate is subducted. The letter A marks a particular material element.

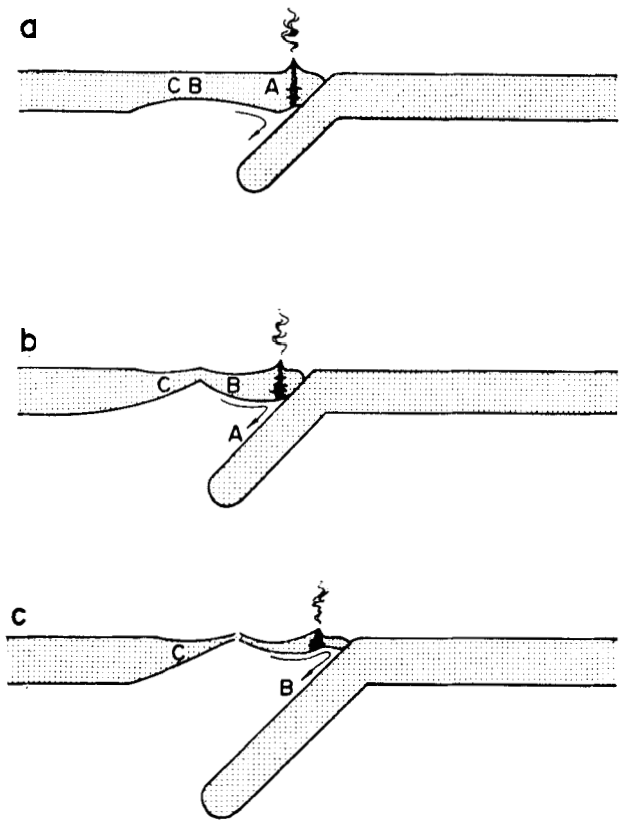

FIG. 8. A schematic model supported by these calculations. The denser portion of the island-arc plate is subducted. Letters mark particular material elements.

Conclusions

The separate calculations prevented examination of the essential connections between marginal basin spreading and island arc volcanism. The location of the original rifting is not well determined, and there is the possibility that the original rifting might occur at the volcanic chain, as observed (Karig 1971). The ablation is well developed within 2 My while the spreading takes 4 My to develop significantly. Since the volcanics may begin first, the line of volcanoes may be the preferred location for spreading to start. A schematic model based on this idea is shown in Fig. 7. Rifting starts at the site of the volcanic intrusion and the spreading is analogous to that at a mid-ocean ridge. Upwelling material accretes symmetrically, so that the spreading centre migrates away from the trench. The volcanoes, however, remain fixed relative to the trench, above the location where magma can segregate from a mush with a small percentage of melt. It is assumed in the figure that the low density of the island arc crust prevents subduction of any part of the island arc plate. Fig. 8 shows an alternate schematic model, based more closely on the calculations. In this case, rifting begins some point landward of the island arc. The portion of the plate adjacent to the slab is slowly subducted with the slab.

Given the current ignorance of mantle processes, the calculations presented above are useful in illustrating the processes which were inferred to occur beneath island arcs. The models are too idealized to confirm anything other than the feasibility of induced flow as a working hypothesis. More sophisticated calculations must explicitly include

both sides of the subduction zone, the low density of the island arc, and weakening of the lithosphere by volcanic intrusions. It is hoped that this paper will form a basis on which to build these models.

Acknowledgments

The authors are grateful for discussions with Professors S. Uyeda and Nafi Toksöz.

This research was sponsored by the Air Force Cambridge Research Laboratories, Air Force System Command under Contract F19628–72–C–0094.

Department of Earth and Planetary Science
Massachusetts Institute of Technology
Cambridge, Massachusetts 02139

References

Andrews, D. J., 1972. Numerical simulation of sea-floor spreading, *J. geophys. Res.*, **77,** 6470.

Batchelor, G. K., 1967. *An introduction to fluid dynamics*, 224 p., Cambridge University Press, Cambridge.

Gorshkov, G., 1969. Geophysics and petrochemistry of andesite volcanism of the circum-Pacific belt, in *Proceedings of the Andesite Conference, Ore Dept. Geol. Mineral Industries Bull.*, **65,** 91–98.

Gorshkov, G., 1970. *Volcanism and the upper mantle; investigations in the Kurile Island area*, Plenum Press, New York, 385 pp. (English trans.).

Green, T. & Ringwood, A., 1968. Origin of garnet phenocrysts in calc-alkaline rocks, *Contr. Miner. Petrol.*, **18,** 163–174.

Hasebe, K., Fujii, N. & Uyeda, S., 1970. Thermal processes under island arcs, *Tectonophysics*, **10,** 335.

Holmes, A., 1965. *Principles of physical geology*, Nelson, London.

Isacks, B., Oliver, J. & Sykes, L., 1968. Seismology and the new global tectonics, *J. geophys. Res.*, **73,** 5855.

Kanamori, H., 1971. Great earthquakes at island arcs and the lithosphere, *Tectonophysics*, **12,** 187–198.

Karig, D. E., 1971. Origin and development of marginal basins in the western Pacific, *J. geophys. Res.*, **76,** 2542–2561.

Kraus, E., 1971. *Die Entwicklungsgeschichte der Kontinent und Ozeane*, Akademie-Verlag, Berlin, 429 pp.

Matsuda, T. & Uyeda, S., 1971. On the Pacific type orogeny and its model-extension of paired belts concept and possible origin of marginal seas, *Tectonophysics*, **11,** 5–27.

McBirney, A. & Weill, D., 1966. Rhyolite magmas of Central America, *Bull. Volcanol.*, **29,** 435–448.

McKenzie, D., 1969. Speculations on the consequences and causes of plate motions, *Geophys. J. R. astr. Soc.*, **18,** 1–32.

McKenzie, D. & Sclater, J., 1968. Heat flow inside the island arcs of the northwest Pacific, *J. geophys. Res.*, **73,** 3137.

Minear, J. & Toksöz, N., 1970a. Thermal regime of a downgoing slab and new global tectonics, *J. geophys. Res.*, **75,** 1397.

Minear, J. & Toksöz, N., 1970b. Thermal regime of a downgoing slab, *Tectonophysics*, **10,** 367–390.

Molnar, P. & Wyss, M., 1972. Moments, source dimension and stress drops of shallow focus earthquakes in the Tonga–Kermadec arc, *Phys. Earth Planet. Int.*, **6,** 263–278.

Osborn, E., 1969. The complementariness of orogenic andesite and alpine peridotite, *Geochim Cosmochim Acta*, **33,** 307–324.

Oversby, V. & Ewart, A., 1972. Lead isotopic compositions of Tonga–Kermadec volcanics and their petrogenetic significance, *Contr. Mineral. Petrol.*, **37,** 181–210.

Oxburgh, E. & Turcotte, D., 1971. Origin of paired metamorphic belts and crustal dilation in island arc regions, *J. geophys. Res.*, **76,** 1315–1327.

Pushkar, P., McBirney, A. & Kudo, A., 1972. The isotopic composition of strontium in Central American ignimbrites, *Bull. Volcanol.*, **35,** 265–294.

Sclater, J. G., Ritter, U. G. & Dixon, F. S., 1972. Heat flow in the south-western Pacific, *J. geophys. Res.*, **77,** 5697–5704.

Sleep, N. H., 1974. Segregation of magma from mostly crystalline mush, *Bull. geol. Soc. Amer.*, **85,** August.

Sleep, N. & Toksöz, N., 1971. Evolution of marginal basins, *Nature*, **233,** 548.

Sugimura, A. & Uyeda, S., 1973. *Island arcs: Japan and its environs*, Elsevier, Amsterdam, 247 pp.

Toksöz, M. N., Minear, J. & Julian, B., 1971. Temperature field and geophysical effects of a downgoing slab, *J. geophys. Res.*, **76,** 1113–1138.

Turcotte, D. & Schubert, G., 1973. Frictional heating of the descending lithosphere, *J. geophys. Res.*, **78,** 5876–5886.

Utsu, T., 1971. Seismological evidence for anomalous structure of island arcs with special reference to the Japanese region, *Rev. geophys. space Phys.*, **9,** 839–890.

Weertman, J., 1971. Theory of water-filled crevasses in glaciers applied to vertical magma transport beneath oceanic ridges, *J. geophys. Res.*, **76,** 1171–1183.

Appendix I

More on the friction heating hypothesis

The ablation hypothesis has another advantage over the frictional heating mechanism in that the source region of the magma would automatically be compatible with the lithospheric depths of melt segregation inferred from experimental petrology (Green & Ringwood 1968). The proponents of frictional heating have proposed complicated mechanisms to get the melt to segregate at the inferred shallow depth rather than at 100 to 200 km depth near the slab. One hypothesis has been that diapirs of hot material ascend from the slab and melt nearer the surface (Green & Ringwood 1968; Oxburgh & Turcotte 1971). The physical difficulty inherent in this mechanism is that the wedge above the slab must be unstable to small scale convective flow (the diapirs) from heat generated above the slab, yet at the same time be so resistive of the large scale flow that great amounts of frictional heating are generated. A mechanism of partial zone melting by Sugimura & Uyeda (1973) avoids this difficulty at least overtly but would require a fair amount of melt to work.

The observation can be easily quantified by considering a planar slip zone on top of the slab. Shear strain rate in the slip zone is

$$\tau = \eta v/h \tag{I.1}$$

where

τ = shear stress,

η = viscosity,

v = velocity of slab,

h = thickness of slip zone.

If the viscosity is taken as that in the wedge above the slab, the maximum obtainable stress is obtained, since the development of a shear zone can only lower stress. We also note that the critical Rayleigh number for convection, about 2000, must be exceeded if thermal diapirs can rise.

$$R = \rho g \alpha \Delta T h^3 / \eta k > 2000 \tag{I.2}$$

where

ρg = specific weight, 3×10^3 dyne cm^{-3},

α = coefficient of thermal expansion, 5×10^{-5} °C^{-1},

ΔT = temperature difference,

k = thermal diffusivity, 10^{-2} cm^2 s^{-1}.

A minimum shear stress of about 2 kb is needed to overcome the heat conducted into the slab and produce a positive temperature anomaly. Substituting this value into equation (I.1) to determine viscosity and assuming $h = 100$ km and $v = 10$ cm/yr we find that 10^4 °C temperature difference is needed to satisfy inequality (I.2). This amount is clearly so excessive that convection from frictional heating on the slab is precluded. The case against the rise of thermal diapirs from the slab could be made stronger, since these parameters were chosen to maximize the chance of local convection, since the downgoing part of the large scale flow surely retards local convection, and since a finite amplitude of convection requiring a much larger Rayleigh number would be necessary for the thermal diapirs to disrupt the lithosphere.

Appendix II

A short description of the numerical procedure

At each moment of time the stress deviator components, s_{xx} and s_{xy}, must be in static equilibrium,

$$2\frac{\partial^2}{\partial x \partial y} s_{xx} + \left(\frac{\partial^2}{\partial y^2} - \frac{\partial^2}{\partial x^2}\right) s_{xy} + \frac{\partial(\rho g)}{\partial x} = 0. \tag{II.1}$$

In the case of linear viscosity, the stress deviator components are related to stream function by

$$s_{xx} = 2\eta \frac{\partial^2 S}{\partial x \partial y} \tag{II.2}$$

$$s_{xy} = \eta \left(\frac{\partial^2 S}{\partial y^2} - \frac{\partial^2 S}{\partial x^2}\right) \tag{II.3}$$

where the viscosity, η, may depend on temperature and depth. Equations (II.1), (II.2) and (II.3) may be combined to get a generalized biharmonic equation for stream function. A finite difference analogue of that equation is used to solve for stream function by an iterative procedure.

If a yield stress is imposed, the second invariant of the stress deviator tensor should satisfy the inequality

$$s_{xx}^2 + s_{yy}^2 \leqslant Y^2. \tag{II.4}$$

The yield condition can be incorporated into the linear iterative procedure, while maintaining a covariant relation between the stress and strain-rate tensors, by adjusting the viscosity. If the inequality (II.4) is not satisfied, then the value of viscosity found from the constitutive relation is reduced to a smaller effective value, such that equality holds in equation (II.4). This adjustment is not made in every iteration, but only after fairly good convergence is achieved for the effective linear problem resulting from the previous adjustment.

After convergence to stress equilibrium is achieved at a particular time, the temperature field is advanced a step in time, taking into account conduction, advection, frictional heating, and adiabatic temperature changes. Then new values of viscosity are found, and the iteration is repeated to find the new flow field.